HHS Public Access

Author manuscript

Nat Struct Mol Biol. Author manuscript; available in PMC 2013 May 01.

Published in final edited form as:

Nat Struct Mol Biol. 2012 November ; 19(11): 1147–1154. doi:10.1038/nsmb.2388.

Structure of a topoisomerase II-DNA-nucleotide complex reveals a new control mechanism for ATPase activity

Bryan H. Schmidt[1], **Neil Osheroff**[2], and **James M. Berger**[1]

[1]Department of Molecular & Cell Biology, University of California, Berkeley, California, USA

[2]Departments of Biochemistry and Medicine (Hematology/Oncology), Vanderbilt University School of Medicine, Nashville, Tennessee, USA

Abstract

Type IIA topoisomerases control DNA supercoiling and disentangle chromosomes by a complex, ATP-dependent strand passage mechanism. Although a general framework exists for type IIA topoisomerase function, the architecture of the full-length enzyme has remained undefined. Here we present the first structure of a fully-catalytic *Saccharomyces cerevisiae* topoisomerase II homodimer, complexed with DNA and a nonhydrolyzable ATP analog. The enzyme adopts a domain-swapped configuration wherein the ATPase domain of one protomer sits atop the nucleolytic region of its partner subunit. This organization produces an unexpected interaction between the bound DNA and a conformational transducing element in the ATPase domain, which we show is critical for both DNA-stimulated ATP hydrolysis and global topoisomerase activity. Our data indicate that the ATPase domains pivot about each other to ensure unidirectional strand passage and that this state senses bound DNA to promote ATP turnover and enzyme reset.

Keywords

Topoisomerase; supercoiling; ATPase; DNA topology; DNA replication; chromosome segregation

Introduction

Elaborate, multi-protein assemblies serve myriad, vital cellular roles throughout biology[1]. Typically composed of a diverse suite of distinct types of catalytic folds and scaffolding elements, these so-called “molecular machines” collate and coordinate distinct functional activities as a means to link and streamline complex biochemical transactions. Although the role and action of different classes of molecular machines are both diverse and varied, many

Correspondence should be addressed to J.M. (jmberger@berkeley.edu).

Accession codes. Protein Data Bank: Coordinates and structure factors for the structure have been deposited with accession code 4GFH.

Author contributions

B.H.S. and J.M.B. and N.O. designed the experiments. B.H.S. performed all of the experiments. B.H.S. and J.M.B. wrote the paper.

Competing financial interests

The authors declare no competing financial interests.

such systems exhibit highly-articulated movements that are driven by ligand-binding and exchange events. The conversion of nucleoside triphosphates into directed motion and force is a particularly prevalent theme among these systems. How the various components comprising a given machine are organized into higher-order structures, and how such elements coordinate their respective catalytic functions, are outstanding questions in biology.

Type II topoisomerases are archetypal, nucleic acid-remodeling enzymes[2]. Using ATP as a cofactor, different type II topoisomerase family members can variously add or remove DNA supercoils, and either form or unlink DNA tangles and knots. These topological rearrangements rely on a multi-stage mechanism that involves the controlled association and dissociation of distinct subunit dimerization interfaces, or "gates," which help guide the physical movement of one DNA duplex through another[3–7]. The type IIA topoisomerases, found predominantly in bacteria and eukaryotes, possess three such interfaces, termed the N-gate, DNA-gate, and C-gate (Fig. 1a)[2]. In the type IIA reaction cycle, one double-stranded DNA (termed the "G-segment") is bound and cleaved by the enzyme, while a second duplex (the "T-segment") is transported through the break[8]. G-segment breakage is catalyzed by a pair of symmetrically-related tyrosines[9,10], in conjunction with a Mg^{2+} ion-binding Topoisomerase/Primase (TOPRIM) fold[11], forming a transient covalent topoisomerase•DNA cleavage complex. Strand passage is coordinated by defined ATPase domains[12–14] which use ATP binding and hydrolysis to promote T-segment capture, stimulate G-segment cleavage, and coordinate successive opening and closing of the gates[3,8,15,16].

Despite extensive study, a number of fundamental questions persist regarding both the configuration of the type IIA topoisomerase holoenzyme and the coordination of the enzyme catalytic cycle by ATP. Although crystal structures of isolated ATPase and DNA-binding and cleavage regions of these enzymes have been reported (e.g., [5–7,17]), how these elements are juxtaposed with respect to each other remains unknown. Mechanistically, how DNA binding stimulates ATP turnover[18–20], or why ATP hydrolysis is sequential rather than synchronous (at least in yeast topoisomerase II)[21], likewise has been difficult to explain at a structural or biochemical level. Given that type II topoisomerases are members of the broader pantheon of GHKL-family ATPases[22], a group that includes MutL-family DNA repair proteins and Hsp90-type chaperones, answers to these questions are likely to broadly resonate across diverse biochemical systems.

To define the global architecture of a type IIA topoisomerase holoenzyme, we determined the crystal structure of a fully-functional construct of *S. cerevisiae* topo II trapped in a covalent cleavage complex with a G-segment DNA and the non-hydrolyzable ATP analog, AMPPNP. The structure not only definitively establishes the relative juxtaposition between the ATPase regions and the DNA binding-and-cleavage core of the protein, but also reveals two unexpected, higher-order organizational features: a double domain-swapping event between ATPase subunits that forms a topological barrier to strand passage, and an interaction between the highly-bent G-segment and a lysine-rich loop in the ATPase domain. Biochemical studies validate the ATPase-DNA interaction, showing that it is not only critical for activity in both yeast and human topo IIα, but that it serves as a communication

relay that couples DNA binding to the stimulation of ATP turnover. Together, these findings point to the existence of new and hitherto unsuspected intermediate states in the type IIA topoisomerase strand passage cycle, and highlight how discrete functional activities can be coordinated across long distances in a large macromolecular system.

Results

Structure of a functional topo II-DNA-AMPPNP complex

One impediment to imaging the ATPase and DNA-binding and cleavage elements of type IIA topoisomerases in conjunction with each other derives from the large size and dynamic nature of these enzymes. In particular, the three dimerization interfaces can each exist in an associated or dissociated state, giving rise to significant conformational variability within a population. To capture a minimally flexible state, we first used a nicked DNA oligonucleotide containing a single phosphorothiolate site as a suicide substrate to trap a covalent cleavage complex with a functional *S. cerevisiae* topo II construct comprising amino acids 1-1177 (Fig. 1a, Supplementary Fig. 1; Methods). Prior studies of covalent type IIA topoisomerase-DNA complexes using either this type of substrate or a drug-inhibited state have found that formation of the phosphotyrosyl linkage coincides with closure of the DNA-gate and C-gate of the enzyme[23–29]. We then added the non-hydrolyzable ATP analog, AMPPNP, which is known to lock the ATPase gate into its dimerized, clamped form[3,5], as a means to promote association of all three interfaces. Crystals grown from this complex belonged to the space group $P2_12_12_1$ and permitted the collection of diffraction data to 4.4 Å resolution. Subsequent rounds of molecular replacement (MR) using single protomers of the isolated yeast topo II cleavage core and ATPase domain produced a solution that recapitulated a full topo II dimer in the asymmetric unit. Because of the moderate resolution of the data, side-chain positions were generally left in the position found in the original search model during refinement (**Methods**). Despite these relatively modest adjustments, the final structure was readily refined to an R_{work}/R_{free} of 24.0/27.7% with good stereochemistry (Fig. 1b, Table 1, **Methods**). Notably, the dimeric conformations of the ATPase domain and DNA binding and cleavage core in holoenzyme match those seen for the two regions observed in isolation, indicating that these structural states correspond to commonly-populated intermediates in the topo II reaction cycle (Supplementary Fig. 2).

Topo II ATPase elements domain-swap to contact DNA

Organizational models for full-length type IIA topoisomerases have generally speculated that the ATPase domains arch over the G-segment binding surface[6,30,31]. The actual orientation between the two regions has been the subject of speculation, however, both because the two functional elements are connected by a flexible and proteolytically-sensitive linker[12–14], and because structures of the isolated ATPase domains have exhibited a crossover at their extreme C-termini whose relevance has remained uncertain[5,17,32–34]. Our model shows the ATPase domains do indeed sit atop the site of G-segment association and cleavage, but that the central cavity of the ATPase domain dimer is offset by approximately 45° from the hole that runs between the DNA- and C-gates (Fig. 1b). Interestingly, the juxtaposition of the domains appears to give rise to a domain-swapping event, such that the

ATPase region of one protomer contacts the TOPRIM fold of its associated partner subunit (Supplementary Fig. 3).

In addition to domain-swapping, the topo II configuration present in the crystal exhibits a second, distinctive feature: an apparent contact between the ATPase "transducer" subdomain and the backbone of the bent G-segment DNA (Figs. 1, 2a). A closer view of this region highlights a loop that emanates from the outer edge of the transducer domain to take up a position proximal to the DNA backbone. The amino acid sequence conservation of this region, hereafter termed the "K-loop," is somewhat variable among type IIA topoisomerases, but retains up to six consecutive lysines, several of which are well conserved among eukaryotic topo II homologs (Fig. 2b). In previous, higher-resolution structures of the isolated ATPase domains of yeast and human topo IIα, the K-loop has been disordered and unmodeled[17,34]. By contrast, the peptide chain is readily visible in electron density for both protomers seen here (Fig. 2a). Although the resolution of our structure precludes precise modeling of side chain rotomers, the appearance of electron density for the K-loop main chain suggests that this region becomes ordered upon engaging DNA. Our structure also suggests that there may exist additional contacts between each transducer domain and both the TOPRIM and "tower" domains of its symmetry-related protomer; however, the resolution of our data does not permit us to definitively model specific interactions between these elements.

The K-loop is important for DNA strand passage activities

To our knowledge, a functional role for the K-loop *per se* has not been established previously. A prior study had shown that deleting 57-residue region of the transducer region encompassing the K-loop eliminates DNA-stimulated ATPase activity[35], but the molecular basis for this effect was not determined. To test whether specific contacts between the K-loop and DNA might be important for topo II activity, we replaced various lysines in this stretch of the *S. cerevisiae* enzyme with either alanine or glutamate, and examined the ability of the mutant constructs to relax negatively-supercoiled DNA. In this assay, purified plasmid is incubated with a fixed starting level of ATP and increasing concentrations of topo II, after which the reaction products are analyzed by agarose gel electrophoresis (**Methods**). The appearance of discrete DNA topoisomers that migrate more slowly than the starting supercoiled substrate is a hallmark of the DNA relaxation reaction catalyzed by type II topoisomerases other than DNA gyrase[36].

We initially found that single K→A mutations at each of the six lysines in this region did not noticeably affect supercoil relaxation (not shown). However, stronger effects became apparent as individual mutations were combined, with a construct bearing a quadruple KKKK→AAAA mutation in the first four amino acids of the K-loop displaying approximately one-fourth the level of supercoil relaxation activity (Fig. 3a). Because any interaction between the K-loop and DNA is likely to rely on a significant electrostatic component, we reasoned that introducing negative charges at the most highly conserved lysine positions might more significantly impact topo II activity. We therefore prepared a KKKK→AEEA mutant, in which the two most highly-conserved lysines were replaced with glutamates. This mutant exhibits less than 10% the specific activity of the wild-type enzyme

(Fig. 3a). Importantly, both the AEEA protein and its AAAA counterpart could be expressed and purified under identical conditions compared to wild-type topo II, and showed no abnormal migration behavior by size-exclusion chromatography (Supplementary Fig. 4, **Methods**), indicating that the loss of activity displayed by the mutants is not due to folding or assembly defects. Interestingly, the relative distributions of topoisomer populations differ between the mutant and wild-type proteins, suggesting that K-loop integrity may play a role in enzyme processivity.

S. cerevisiae topo II is unusual among eukaryotic type IIA topoisomerases in that it bears six lysines in its K-loop; most other orthologs possess three, including the two that appear universally conserved from yeast to human (Fig. 2b). To determine whether the observed effects of K-loop substitutions on DNA supercoiling were generalizable, we cloned, expressed, and purified the KKK→AAA and KKK→EEE triple mutants of human topo IIα. Negative-supercoil relaxation assays were carried out and analyzed for the mutant and wild type topo IIα proteins as for yeast topo II. The resultant data show that both mutants impede the removal of supercoils, with the lysine-to-glutamate charge substitutions again exhibiting a more severe defect in activity compared to the alanine substitutions (Supplementary Fig. 5a–b). Thus, the K-loop appears to play a part in strand passage across different topo II orthologs.

To more precisely define the action of the K-loop, we examined DNA decatenation by yeast topo II and the K-loop mutants. Decatenation can be assessed by incubating purified enzyme with kinetoplast DNA (kDNA) and ATP, and then resolving the products by agarose gel electrophoresis. kDNA normally comprises a large, catenated network of minicircles that cannot enter a standard agarose gel; however, the unlinking action of a type II topoisomerase produces individual minicircles that migrate freely into the matrix[37]. Using this assay, we found that the AAAA and AEEA mutants display reduced levels of activity comparable to those seen during supercoil relaxation (Fig 4a). These results show that the role of the K-loop is not restricted to the type of DNA substrate encountered by topo II, but is instead necessary to support strand passage overall.

Because defects in strand passage could arise from an impaired ability to cleave DNA, we next set out to investigate the strand scission properties of the enzyme. Cleavage was examined by first incubating yeast topo II with negatively-supercoiled plasmid DNA in the presence of AMPPNP and either Mg^{2+} or Ca^{2+} ions, followed by rapid denaturation of the complex with SDS and resolution of the products on an agarose gel. Ca^{2+} is known to stimulate cleavage over background levels of cutting[38], resulting a species that comigrates with linearized vector. Notably, both the AAAA and AEEA mutants produce similar amounts of linear DNA as the wild-type enzyme (Fig. 4b). These results support the position that topo II K-loop mutants are not generally compromised by a folding or assembly defect, and that the integrity of this region is necessary to support the strand passage reaction following G-segment binding and cleavage.

The K-loop couples DNA binding to ATPase activity

Loss of supercoil relaxation and decatenation activities can in principle arise from a deficiency in one of any number of steps in the type IIA topoisomerase catalytic cycle.

Having established that DNA cleavage appears unperturbed in our K-loop mutants, we next examined the ATPase activity of enzyme. The transducer subdomain on which the K-loop resides is known to play a key role in ATP hydrolysis by providing an invariant amino acid (Lys367 in yeast topo II) that plugs into the GHKL nucleotide-binding pocket. Although the K-loop sits ~50 Å away from this active site residue, residing instead on the outer edge of the ATPase region (Fig. 1b), we reasoned that it might nonetheless indirectly influence nucleotide turnover at a distance. Using an established, coupled assay to report on ATPase function[39,40], we first assessed the basal ATPase rates between the WT, AAAA, and AEEA topo II constructs. The overall profiles of all three proteins are similar (Fig. 5a), with the AEEA actually exhibiting a slightly greater level of specific activity than the other two enzymes. The V_{max} and K_M values obtained from these curves also are similar (Table 2) and in line with values reported previously for the WT yeast enzyme[19]. Hence, the intrinsic ATPase activity of topo II does not appear to be compromised by K-loop alterations, again indicating that the substitutions do not directly impair the folding or function of the domain.

By contrast, the influence of DNA on the ATPase rate of mutant enzymes is striking. It has been well established that DNA stimulates ATP turnover by more than an order of magnitude in most type IIA topoisomerases studied to date[18–20,41]. To assess this effect for our K-loop mutants, we measured ATPase rates at a single starting ATP concentration in the presence of increasing amounts of sheared salmon-sperm DNA. The ATPase activity of our wild-type topo II preparations is stimulated ~15 fold in this assay(Fig. 5b), a level consistent with prior measurements for this enzyme *in vitro* [19]. By contrast, both the AAAA and AEEA topo II mutants failed to exhibit stimulation upon the addition of DNA (Fig. 5b). To ensure that this effect was not limited to the yeast enzyme, we measured whether DNA could stimulate the activity of human topo IIα. Consistent with prior observations[42,43], the degree of enhancement observed for our wild-type topo IIα protein is ~20-fold; however, DNA only doubles the ATPase activity of the two topo IIα K-loop mutants (Supplementary Fig. 5c–d). Together, these data indicate that the K-loop plays an unexpected but direct role in coupling DNA binding with ATP turnover and strand passage.

Inspection of our crystal structure shows that that the K-loop appears to interact with a DNA region that flanks the nucleolytic center and site of DNA bending (Fig. 1c, 2a). If the K-loop indeed allows the ATPase activity of topo II to sense whether DNA is stably associated with the enzyme, then the nature of this contact predicts that sensing should be dependent on the length of the G-segment associated with the primary DNA binding and cleavage center; i.e., oligonucleotides shorter than 30 bp should not be long enough to reach the K-loop and thus should stimulate ATPase rates only minimally, whereas longer oligonucleotides should extend past the ATPase domain and allow contact to occur. To test this assumption, we investigated the role of DNA oligonucleotide length on the stimulation of ATPase rate. A series of oligonucleotides, ranging from 20–70bp and each containing a centered, preferred site for topo II binding[44], were individually added to ATPase reactions containing WT topo II, and their effects monitored as a function of turnover rate. Notably, the intact 20mer substrate was unable to appreciably stimulate ATP turnover, even at a saturating molar ratio (250:1) of DNA:enzyme. By contrast, as the length of the intact oligonucleotides was increased at a constant DNA concentration, the ATPase activity of the enzyme also

increased (Fig. 6, Supplementary Fig. 6). These findings are consistent with the concept that a bound G-segment DNA needs to be of a certain length to reach the ATPase domains and their associated K-loops.

Discussion

A complete topo II-DNA-nucleotide structure

Despite a general acceptance by the community, the structural organization of a fully-functional type IIA topoisomerase has not been established. The work described here fills this gap, resolving the question of how the ATPase domains connect with the rest of the enzyme (Fig. 1). The only part of the enzyme missing in our construct is a poorly-conserved C-terminal region (residues 1178-1428), which contains both phosphorylation and nuclear localization sites[45,46]. In human topo IIα, this element plays a role in the stimulating the relaxation of positive supercoils. However, this region is not required for negative-supercoil relaxation, nor are its stimulatory properties retained by its paralog, topo IIβ[47]. Moreover, deletion of the C-terminus of *S. cerevisiae* topo II has no effect on DNA strand passage compared to the full-length protein *in vitro*[48]. Hence, our structure reflects a minimal type IIA topoisomerase variant that possesses all of the elements necessary to support normal strand passage activities.

One notable feature of our full-length model – which derives from a complete view of the topo II holoenzyme in the crystal – is that its two major functional parts, the ATPase domains and the DNA-binding and cleavage core, adopt dimeric conformational states that are essentially indistinguishable from structures of the same regions in isolation from each other (Supplementary Fig. 2)[17,27]. This finding supports the biological relevance of these and other fragment-derived models to understanding type IIA topoisomerase mechanism as a whole. In particular, we note the interior hole formed between the dimerized topo II ATPase domains remains much smaller than is seen for the equivalent regions of bacterial type IIA enzymes (Supplementary Fig. 2)[5,17,32–34]. This finding is noteworthy because the size of this feature in topo II would appear to preclude the stable binding and trapping of DNA in its nucleotide-bound form. This observation likely accounts for the known inability of yeast topo II to accommodate a T-segment prior to DNA-gate opening[49].

Intriguingly, nearly all dimerized type IIA topoisomerase ATPase domain models visualized to date have displayed an intertwined structure that results from domain swapping events at both the N- and C-termini (Supplementary Fig. 2)[5,17,32–34]. While the significance of this doubly-wrapped configuration has remained unclear, particularly insofar as the modest contact seen at the extreme C-terminus, we note that it is preserved in the DNA- and AMPPNP-bound topo II structure observed here (Supplementary Fig. 3). This consistency strongly argues that the reciprocal exchange of ATPase domain elements is a universal feature of type IIA topoisomerases that reflects a specific intermediate in the catalytic cycle. Interestingly, this domain-swapping event leads to the topological segregation of the upper ATPase domain hole from the G-segment binding surface. Taken together with the small interior hole manifest by the dimerized topo II ATPase domains, these physical features suggest that our model most likely corresponds to a state that follows both nucleotide binding and T-segment transport. Consistent with this proposal, biochemical studies of yeast

topo II have shown that AMPPNP can support a single, complete round of DNA passage, but that the ATPase domains remain dimerized, preventing further rounds of activity[8,50,51].

A direct connection between the ATPase elements and DNA

The coupling between DNA binding and ATP turnover is of the most enigmatic aspects of type II topoisomerase function, and of many nucleic-acid dependent motors in general. A particularly unexpected feature of the ternary complex imaged here is the appearance of a direct connection between the ATPase "transducer" subdomain and the bound G-segment DNA (Fig. 2). Site-directed mutagenesis of conserved lysines in this region of both yeast topo II and human topo IIα did not appreciably affect DNA cleavage, but did adversely impact both DNA decatenation and supercoil relaxation activity (Figs. 3, 4, Supplementary Fig. 5a–b). Moreover, the K-loop mutations resulted in essentially a complete loss of DNA-stimulated ATPase activity, without affecting basal ATP turnover rates (Fig. 5, Supplementary Fig. 5c–d). These data indicate that the K-loop•DNA interaction we observe occurs in solution and that the K-loop itself is a hitherto unanticipated control element for coupling DNA binding with nucleotide hydrolysis at a distance. They also establish DNA as a conduit for linking the site of G-segment binding and bending with catalysis by the ATPase centers of the enzyme.

The dependence of DNA length in stimulating ATPase activity further corroborates the K-loop•G-segment interaction (Fig. 6). Whereas the stimulatory effect of a 20mer oligonucleotide substrate on hydrolysis rates is negligible, even when present in vast excess over enzyme, increasing DNA length results in progressively greater activity. Crystal structures have shown that 20mer duplexes can be bound and cleaved by the G-segment binding core[23,26]; however, these substrates do not extend far enough out of the active site to engage the K-loop. Notably, longer oligonucleotide substrates do not approach the stimulatory effect of sheared salmon-sperm DNA (Figs. 5b, 6), whose average length is on the order of hundreds of base pairs. This result suggests that while the K-loop•G-segment interaction directly contributes to ATPase stimulation, the interaction by itself is not sufficient to account for the full stimulation by DNA on ATPase rates. As previous work has implicated T-segment binding to the ATPase in stimulating ATPase activity[42,52], it is possible that salmon sperm DNA is more greatly stimulatory because it is sufficiently long to serve as both a G- and T-segment. Alternatively (or in addition), there may exist additional contacts between G-segment DNA and the transducer or GHKL ATPase fold further up the domain that our structure does not reveal due to the short length (30 bp) of our DNA.

An inspection of the literature provides additional support for the K-loop•DNA contact that we observe. A prior protein "footprinting" study using *S. cerevisiae* topo II identified five lysines that become protected upon binding DNA[53]. Four of these residues lie in the major DNA binding groove of the catalytic core and are masked by the associated G-segment; however, the fifth lysine was found to reside on the K-loop. Although a role for this region was not known at the time of this effort, the authors speculated that protection within this region might have resulted from a conformational change or from direct DNA interactions – the present work indicates that it is both. In a second, more recent investigation, high-

throughput mass spectrometry revealed that human topo IIβ is subject to acetylation[54]. Interestingly, three acetylation sites were discovered, all of which either reside on or are proximal to the K-loop region (K365, K367, and K373 in hTop2β numbering). The biological significance of modifying these residues, if any, is not known, but based on the findings described here, might serve as a specific means for regulating topo IIβ activity inside the cell.

Complexities in type IIA topoisomerase strand-passage

If the structure reported here corresponds to a functional intermediate in the topo II strand passage cycle, then what might be purpose for the domain swapping we observe between ATPase domain elements? In the current, generalized version of the type IIA topoisomerase catalytic cycle, both a G-and a T-segment must be captured by the enzyme prior to ATP binding (Fig. 7)[3,6,8,30]. Nucleotide association drives dimerization of the ATPase domains, along with the cleavage and opening of the G-segment, and passage of the T-segment through the break. During passage, the T-segment DNA is generally considered to transit exclusively from the N-terminal portion of the protein to its C-terminal side[4,16]. Unidirectionality is thermodynamically aided by the consumption of ATP[55]; however, the mechanical motions that enforce one-way movement have been ill-defined. The ability of the ATPase domains to wrap around themselves provides one possible solution to this problem, as a crossover of the protein chain would provide a physical impediment to movement of the T-segment back through the cleaved G-segment once passage has occurred. We note that this scheme would require the dimerized ATPase domains to twist about each other by perhaps as much as 180° before “locking” into place against the G-segment following transport (Fig. 7). Although extreme, an inspection of the ATP-dimerized Hsp90 chaperone, which employs the same family of ATPase fold as topo II, intertwines around itself to a similar extent (Supplementary Fig. 7)[56].

Our structure raises a second unanticipated issue involving type IIA topoisomerase mechanism, namely, why these enzymes might have evolved a contact that allows the ATPase domains to sense the presence of a properly bound and bent G-segment *after* strand passage has occurred. One possibility is that this contact affords an extra layer of control to more tightly couple ATP turnover with strand passage. Outside of gyrase, which uses the free energy of ATP to add negative supercoils to DNA[57], the need for ATP in the type IIA topoisomerase reaction has remained enigmatic. One model is that ATP serves as a timing element, or “gatekeeper,” that temporarily promotes the formation of a new dimer interface during DNA cleavage to secure the two DNA ends[55]. Since establishment of the nucleolytic center appears to coincide with a very precisely phased DNA bend[23,25,27,28,58], having the ATPase domains touch the G-segment could help signal that the passage reaction is complete, and that ATP can be hydrolyzed to allow enzyme reset. Consistent with this idea, pre-steady state kinetic studies have shown that the ATPase elements of *S. cerevisiae* topo II fire asynchronously, with one ATP hydrolyzed prior to or concomitant with strand passage, and the other hydrolyzing later, likely after strand passage is complete[21]. These data suggest that the K-loop•DNA interaction we observe may predominantly affect the second ATPase event (Fig. 7). In accord with this reasoning, a human topo IIα heterodimer containing only a single functional ATP-binding site is weakly able to relax DNA supercoils, but shows no

DNA-stimulated ATPase activity[59]; our model would predict that this mutant enzyme can support only the first ATP turnover step that drives strand passage, but not the step required to stimulate enzyme turnover. Similarly, biochemical analyses have indicated that the ATPase activity of *B. subtilis* gyrase, which lacks the K-loop, is not asynchronous[60]. Future studies will be needed to test these concepts further.

Concluding remarks

Type IIA topoisomerases are multisubunit DNA remodeling enzymes that undergo a series of highly-articulated movements to physically move one DNA through another. The structural and biochemical studies reported here definitively establish the higher-order structural organization of this class of enzymes, and further reveal new architectural linkages that help couple ATP turnover with strand passage. These findings highlight some of the unanticipated and sophisticated complexities that can be employed by molecular machines, particularly those that rely or act on nucleic acids, to coordinate disparate catalytic events in support of essential biochemical transactions.

Online Methods

Topo II expression and purification

Residues 1–1177 of *S. cerevisiae* topoisomerase II were expressed as a fusion with an amino-terminal tobacco etch virus (TEV) protease-cleavable hexahistidine (His_6) tag. Prior studies have shown that this construct retains the full catalytic activity of the wild-type protein *in vitro*, but lacks nuclear localization elements that would allow it to complement a *top2* ts allele *in vivo*[48]. Overexpression was carried out in *S. cerevisiae* strain BCY123 grown in complete supplement mixture dropout medium lacking uracil (CSM-URA), supplemented with lactic acid (2%) and glycerol (1.5%) for a carbon source. Galactose (20 g L^{-1}) was added at OD=0.8 for induction (6 h at 30 °C). Induced cells were collected by centrifugation, resuspended in Buffer A (300 mM KCl, 20 mM Tris-HCl (pH 8.5), 10% glycerol, 20 mM imidazole (pH 8.0), 1 mM phenylmethylsulphonyl fluoride), flash frozen in liquid nitrogen, and lysed by grinding under liquid nitrogen. Ground cell powder was resuspended in Buffer A and centrifuged (20 min, 16000 rpm) to clarify the lysate. Protein was purified by tandem nickel-affinity and ion-exchange chromatography (nickel-chelating Sepharose and HiTrap SP, GE), followed by removal of the His_6 tag with His_6-tagged TEV protease and passage over a second nickel affinity column to remove uncleaved protein and the protease. The protein was then run over a gel-filtration column (S-300, GE) equilibrated in 10% glycerol, 500 mM KCl and 20 mM Tris (pH 7.9). Peak fractions were assessed by SDS-PAGE, collected, and concentrated in Amicon 100 kDa cutoff concentrators (Millipore).

Human topo IIα was prepared similarly to the yeast enzyme, but was not tagged with a hexahistidine tag. As such, after resuspension in Buffer A (without imidazole), a 35% ammonium sulfate precipitation step, followed by centrifugation was performed. The resultant supernatant, which contains topo IIα, was subjected to an additional 65% ammonium sulfate cut, after which the protein was spun down in the precipitate. The precipitated protein was resuspended in 100 mM KCl, 20 mM Tris-HCl (pH 8.5), 10%

glycerol, 1 mM phenylmethylsulphonyl fluoride, and flowed over an ion exchange column (HiTrap SP, GE). The protein was eluted with an increasing KCl salt gradient, and then collected and run over a gel-filtration column (S-300, GE) equilibrated in 10% glycerol, 500 mM KCl and 20 mM Tris-Cl (pH 7.9). Peak fractions were assessed by SDS-PAGE, collected, and concentrated in Amicon 100 kDa cutoff concentrators (Millipore).

Covalent complex formation and purification

Both standard and phosphorothiolate oligonucleotides were synthesized on an in-house ABI synthesizer. Phosphorothioamidite for producing the 3′-bridging phosphorothiolate was synthesized as reported[61]. After synthesis, DNAs were purified by running on a 12% denaturing urea-formamide PAGE, illuminating by UV, excising the bands, crushing the gel matrix, and eluting overnight into 500 mM ammonium acetate and 10 mM magnesium acetate. The oligonucleotides were then cleaned with a C18 column (Waters), lyophilized overnight, and resuspended in 10 mM Tris-Cl (pH 7.9) and 200 mM KCl. The oligonucleotide containing the phosphorothiolated bond was mixed with the two shorter oligonucleotides to assemble a singly-nicked substrate (Supplementary Fig. 1), heated to 90°C in a water bath, and cooled to room temperature overnight to anneal. For producing the cleavage complex, annealed oligonucleotides were incubated for 45 min at room temperature at a 1.2:1 molar ratio of oligonucleotide:enzyme in 100 mM KCl, 10 mM Tris (pH 7.9) 5 mM $MnCl_2$, and 1 mM AMPPNP. Unreacted protein, DNA, and nucleotide were separated from the complex by passing the sample over a gel filtration column (S-300, GE) and cation exchange column (HiTrap SP, GE), connected in series and pre-equilibrated with 20 mM Tris (pH 7.9), 100 mM KCl, and 5 mM $MgCl_2$. The gel filtration column removed unbound DNA from the protein, whereas unbound protein and the DNA-cleavage complex were separated by the cation-exchange column. The protein–DNA complex was then concentrated to 5 mg ml^{-1} in the column buffer, with fresh AMPPNP added to 1 mM final concentration.

Crystallization and structure solution

Crystals were grown at 18°C in hanging drop format by mixing 1 μl protein solution with 1 μl well solution containing 23% PEG 300 and 100 mM Tris (pH 8.0). For harvesting, crystals were transferred for one minute to well solution containing 10% xylitol, and then looped and flash frozen in liquid nitrogen. Data were collected at Beamline 8.3.1 (wavelength 1.1159 Å) under a cryo-stream at the Advanced Light Source (ALS) at Lawrence Berkeley National Laboratory, and integrated using HKL2000[62]. Initial phases were calculated by molecular replacement (MR) using two independent search models for PHASER[63]. The first model corresponded to a single, DNA-free promoter from the cleavage complex of the *S. cerevisiae* topo II DNA binding and cleavage core (residues 421–1177 of PDB ID code 3L4J)[27], and the second to one protomer from the *S. cerevisiae* topo II ATPase domain dimer (residues 7-406 of PDB ID code 1PVG)[17]. The final MR solution regenerated one intact holoenzyme dimer in the asymmetric unit and resulted in clear electron density for the duplex DNA substrate in difference maps. Building of the model was carried out in COOT[64], followed by a refinement strategy using PHENIX[65] that consisted of an initial round of rigid-body refinement, followed only by individual-atom and TLS refinement. For individual atom refinement, both secondary structure restraints and NCS restraints were

employed, with refinement parameters weighted to highly favor geometry. This approach kept most side-chain rotamers in their original conformers, improved the model's geometry, better placed the peptide backbone into electron density maps, and markedly improved R_{free}. Structure validation was assisted by MolProbity[66], and figures were rendered using PyMOL[67]. 97.7% of main-chain torsion angles fell within favored regions of Ramachandran space, as calculated by MolProbity, with only 2.3% in allowed regions, and 0% in disallowed.

Notes on structure modeling

Because a non-palindromic DNA sequence was used for co-crystallization (Supplementary Fig. 1), electron density for the DNA corresponded to an average of the two possible sequence orientations. To account for this overlap, we modeled the DNA density as two alternate oligonucleotide segments, each present at half-occupancy. We note that such an approach has been used in similar circumstances[27], and that the DNA sequence orientation does not alter any subsequent analysis or conclusions in this paper.

DNA supercoiling relaxation, decatenation, and cleavage assays

Wild-type or mutant topo II (or topo IIα) was incubated with 300 ng (7.5 μM) negatively-supercoiled pUC19 plasmid DNA or kDNA in 20 μL reactions for 30 min at either 30°C (for the yeast enzyme), or 37°C (human protein). The final reaction conditions included 10 mM Tris pH 7.9, 100 mM KCl, 5 mM $MgCl_2$, 2% glycerol, and 1 mM ATP. Reactions were stopped with the addition of 0.5% SDS and 12.5 mM EDTA (final concentrations), and then treated with proteinase K for 30 minutes at 42°C. Sucrose-based loading dye was added to samples, and samples were run on a 1.2% agarose (Invitrogen), 1X TAE gel at 1–1.5 V cm^{-1} for 16–18 h. Gels were stained with 0.5 μg ml^{-1} ethidium bromide (EtBr) for 20 min, followed by destaining for 30 min. Bands were visualized by UV transillumination.

ATPase assay

Wild-type and mutant topo II ATPase activities were measured using an established enzyme-coupled assay in which the hydrolysis of ATP to ADP is coupled to the oxidation of NADH to NAD+[39,40]. To determine standard kinetic parameters (K_M, V_{max}), 50 nM homodimeric enzyme was incubated with 0–4 mM ATP in 75 μl reactions. Reactions contained 50 mM Tris pH 7.9, 100 mM KCl, 8 mM $MgCl_2$, 5 mM β-mercaptoethanol, 0.2 mg ml^{-1} bovine serum albumin, 2 mM phosphoenol pyruvate (PEP), 0.2 mM β-nicotinamide adenine dinucleotide (NADH), and an excess of pyruvate kinase and lactate dehydrogenase (enzyme mix obtained from Sigma). Assays were performed at 30°C for yeast and 37°C for human enzymes, with the oxidation of NADH to NAD^+ monitored by measuring absorbance at 340 nm in a Perkin Elmer Victor ^{3}V 1420 multilabel plate reader. The rate of decrease in absorbance was converted to μmol of ATP hydrolyzed to ADP using an NADH standard curve and the assumption that one ATP is hydrolyzed for every NADH oxidized. ATPase rate as a function of [ATP] was fit for K_M and V_{max} using Michaelis–Menten kinetics in KaleidaGraph (Synergy Software). DNA stimulation of ATPase activity was measured using assays performed as described, except that the starting concentration of ATP was held constant (0.25 mM for yeast and 1 mM for human), and reactions were

supplemented either with varying amounts of sheared, purified sheared salmon-sperm DNA (Sigma), or with oligonucleotide substrates (IDT); in analyzing ATPase activity measured as a function of salmon-sperm DNA concentration, use of the Hill equation resulted in a much better fit to the observed data than did Michaelis–Menten treatment. In experiments of oligonucleotide-stimulated ATPase rates, oligonucleotides were titrated up to 12.5 μM, a 250:1 molar ratio of oligonucleotide:enzyme, where the stimulative effect of DNA was at a maximum.

Supplementary Material

Refer to Web version on PubMed Central for supplementary material.

Acknowledgments

The authors thank A. Burgin at Emerald BioStructures for synthesizing the phosphorothioamidite reagent, as well as members of the Berger Lab for helpful discussions. This work was supported by a training grant (GM08295 to B.H.S.) and the NCI (CA077373 to J.M.B.) and the NIH (GM33944 to N.O.)

References

1. Bustamante C, Cheng W, Mejia YX. Revisiting the central dogma one molecule at a time. Cell. 2011; 144:480–97. [PubMed: 21335233]
2. Schoeffler AJ, Berger JM. DNA topoisomerases: harnessing and constraining energy to govern chromosome topology. Q Rev Biophys. 2008; 41:41–101. [PubMed: 18755053]
3. Roca J, Wang JC. The capture of a DNA double helix by an ATP-dependent protein clamp: a key step in DNA transport by type II DNA topoisomerases. Cell. 1992; 71:833–40. [PubMed: 1330327]
4. Roca J, Berger JM, Harrison SC, Wang JC. DNA transport by a type II topoisomerase: direct evidence for a two-gate mechanism. Proc Natl Acad Sci U S A. 1996; 93:4057–62. [PubMed: 8633016]
5. Wigley DB, Davies GJ, Dodson EJ, Maxwell A, Dodson G. Crystal structure of an N-terminal fragment of the DNA gyrase B protein. Nature. 1991; 351:624–9. [PubMed: 1646964]
6. Berger JM, Gamblin SJ, Harrison SC, Wang JC. Structure and mechanism of DNA topoisomerase II. Nature. 1996; 379:225–32. [PubMed: 8538787]
7. Morais Cabral JH, Jackson AP, Smith CV, Shikotra N, Maxwell A, Liddington RC. Crystal structure of the breakage-reunion domain of DNA gyrase. Nature. 1997; 388:903–6. [PubMed: 9278055]
8. Roca J, Wang JC. DNA transport by a type II DNA topoisomerase: evidence in favor of a two-gate mechanism. Cell. 1994; 77:609–16. [PubMed: 8187179]
9. Worland ST, Wang JC. Inducible overexpression, purification, and active site mapping of DNA topoisomerase II from the yeast Saccharomyces cerevisiae. J Biol Chem. 1989; 264:4412–6. [PubMed: 2538443]
10. Tse YC, Kirkegaard K, Wang JC. Covalent bonds between protein and DNA. Formation of phosphotyrosine linkage between certain DNA topoisomerases and DNA. J Biol Chem. 1980; 255:5560–5. [PubMed: 6155377]
11. Aravind L, Leipe DD, Koonin EV. Toprim--a conserved catalytic domain in type IA and II topoisomerases, DnaG-type primases, OLD family nucleases and RecR proteins. Nucleic Acids Res. 1998; 26:4205–13. [PubMed: 9722641]
12. Lindsley JE, Wang JC. Study of allosteric communication between protomers by immunotagging. Nature. 1993; 361:749–50. [PubMed: 7680110]
13. Gellert M, Fisher LM, O'Dea MH. DNA gyrase: purification and catalytic properties of a fragment of gyrase B protein. Proc Natl Acad Sci U S A. 1979; 76:6289–93. [PubMed: 230505]

14. Brown PO, Peebles CL, Cozzarelli NR. A topoisomerase from Escherichia coli related to DNA gyrase. Proc Natl Acad Sci U S A. 1979; 76:6110–4. [PubMed: 230498]
15. Williams NL, Maxwell A. Locking the DNA gate of DNA gyrase: investigating the effects on DNA cleavage and ATP hydrolysis. Biochemistry. 1999; 38:14157–64. [PubMed: 10571989]
16. Williams NL, Maxwell A. Probing the two-gate mechanism of DNA gyrase using cysteine cross-linking. Biochemistry. 1999; 38:13502–11. [PubMed: 10521257]
17. Classen S, Olland S, Berger JM. Structure of the topoisomerase II ATPase region and its mechanism of inhibition by the chemotherapeutic agent ICRF-187. Proc Natl Acad Sci U S A. 2003; 100:10629–34. [PubMed: 12963818]
18. Mizuuchi K, O'Dea MH, Gellert M. DNA gyrase: subunit structure and ATPase activity of the purified enzyme. Proc Natl Acad Sci U S A. 1978; 75:5960–3. [PubMed: 153529]
19. Lindsley JE, Wang JC. On the coupling between ATP usage and DNA transport by yeast DNA topoisomerase II. J Biol Chem. 1993; 268:8096–104. [PubMed: 8385137]
20. Osheroff N, Shelton ER, Brutlag DL. DNA topoisomerase II from Drosophila melanogaster. Relaxation of supercoiled DNA. J Biol Chem. 1983; 258:9536–43. [PubMed: 6308011]
21. Harkins TT, Lewis TJ, Lindsley JE. Pre-steady-state analysis of ATP hydrolysis by Saccharomyces cerevisiae DNA topoisomerase II. 2. Kinetic mechanism for the sequential hydrolysis of two ATP. Biochemistry. 1998; 37:7299–312. [PubMed: 9585544]
22. Dutta R, Inouye M. GHKL, an emergent ATPase/kinase superfamily. Trends Biochem Sci. 2000; 25:24–8. [PubMed: 10637609]
23. Laponogov I, et al. Structural basis of gate-DNA breakage and resealing by type II topoisomerases. PLoS One. 2010; 5:e11338. [PubMed: 20596531]
24. Laponogov I, et al. Structural insight into the quinolone-DNA cleavage complex of type IIA topoisomerases. Nat Struct Mol Biol. 2009; 16:667–9. [PubMed: 19448616]
25. Wohlkonig A, et al. Structural basis of quinolone inhibition of type IIA topoisomerases and target-mediated resistance. Nat Struct Mol Biol. 2010; 17:1152–3. [PubMed: 20802486]
26. Bax BD, et al. Type IIA topoisomerase inhibition by a new class of antibacterial agents. Nature. 2010; 466:935–40. [PubMed: 20686482]
27. Schmidt BH, Burgin AB, Deweese JE, Osheroff N, Berger JM. A novel and unified two-metal mechanism for DNA cleavage by type II and IA topoisomerases. Nature. 2010; 465:641–4. [PubMed: 20485342]
28. Wu CC, et al. Structural basis of type II topoisomerase inhibition by the anticancer drug etoposide. Science. 2011; 333:459–62. [PubMed: 21778401]
29. Wendorff TJ, Schmidt BH, Heslop P, Austin CA, Berger JM. The Structure of DNA-Bound Human Topoisomerase II Alpha: Conformational Mechanisms for Coordinating Inter-Subunit Interactions with DNA Cleavage. J Mol Biol. 2012
30. Kampranis SC, Bates AD, Maxwell A. A model for the mechanism of strand passage by DNA gyrase. Proc Natl Acad Sci U S A. 1999; 96:8414–9. [PubMed: 10411889]
31. Schultz P, Olland S, Oudet P, Hancock R. Structure and conformational changes of DNA topoisomerase II visualized by electron microscopy. Proc Natl Acad Sci U S A. 1996; 93:5936–40. [PubMed: 8650197]
32. Lamour V, Hoermann L, Jeltsch JM, Oudet P, Moras D. An open conformation of the Thermus thermophilus gyrase B ATP-binding domain. J Biol Chem. 2002; 277:18947–53. [PubMed: 11850422]
33. Brino L, et al. Dimerization of Escherichia coli DNA-gyrase B provides a structural mechanism for activating the ATPase catalytic center. J Biol Chem. 2000; 275:9468–75. [PubMed: 10734094]
34. Wei H, Ruthenburg AJ, Bechis SK, Verdine GL. Nucleotide-dependent domain movement in the ATPase domain of a human type IIA DNA topoisomerase. J Biol Chem. 2005; 280:37041–7. [PubMed: 16100112]
35. Bjergbaek L, et al. Communication between the ATPase and cleavage/religation domains of human topoisomerase IIalpha. J Biol Chem. 2000; 275:13041–8. [PubMed: 10777608]

36. Liu LF, Liu CC, Alberts BM. Type II DNA topoisomerases: enzymes that can unknot a topologically knotted DNA molecule via a reversible double-strand break. Cell. 1980; 19:697–707. [PubMed: 6244895]
37. Marini JC, Miller KG, Englund PT. Decatenation of kinetoplast DNA by topoisomerases. J Biol Chem. 1980; 255:4976–9. [PubMed: 6246090]
38. Osheroff N, Zechiedrich EL. Calcium-promoted DNA cleavage by eukaryotic topoisomerase II: trapping the covalent enzyme-DNA complex in an active form. Biochemistry. 1987; 26:4303–9. [PubMed: 2822084]
39. Lindsley JE. Use of a real-time, coupled assay to measure the ATPase activity of DNA topoisomerase II. Methods Mol Biol. 2001; 95:57–64. [PubMed: 11089219]
40. Tamura JK, Gellert M. Characterization of the ATP binding site on Escherichia coli DNA gyrase. Affinity labeling of Lys-103 and Lys-110 of the B subunit by pyridoxal 5′-diphospho-5′-adenosine. J Biol Chem. 1990; 265:21342–9. [PubMed: 2174443]
41. Maxwell A, Gellert M. The DNA dependence of the ATPase activity of DNA gyrase. J Biol Chem. 1984; 259:14472–80. [PubMed: 6094559]
42. Hammonds TR, Maxwell A. The DNA dependence of the ATPase activity of human DNA topoisomerase IIalpha. J Biol Chem. 1997; 272:32696–703. [PubMed: 9405488]
43. West KL, Turnbull RM, Willmore E, Lakey JH, Austin CA. Characterisation of the DNA-dependent ATPase activity of human DNA topoisomerase IIbeta: mutation of Ser165 in the ATPase domain reduces the ATPase activity and abolishes the in vivo complementation ability. Nucleic Acids Res. 2002; 30:5416–24. [PubMed: 12490710]
44. Mueller-Planitz F, Herschlag D. DNA topoisomerase II selects DNA cleavage sites based on reactivity rather than binding affinity. Nucleic Acids Res. 2007; 35:3764–73. [PubMed: 17517767]
45. Shiozaki K, Yanagida M. Functional dissection of the phosphorylated termini of fission yeast DNA topoisomerase II. J Cell Biol. 1992; 119:1023–36. [PubMed: 1332977]
46. Cardenas ME, Dang Q, Glover CV, Gasser SM. Casein kinase II phosphorylates the eukaryote-specific C-terminal domain of topoisomerase II in vivo. EMBO J. 1992; 11:1785–96. [PubMed: 1316274]
47. McClendon AK, et al. Bimodal recognition of DNA geometry by human topoisomerase II alpha: preferential relaxation of positively supercoiled DNA requires elements in the C-terminal domain. Biochemistry. 2008; 47:13169–78. [PubMed: 19053267]
48. Caron PR, Watt P, Wang JC. The C-terminal domain of Saccharomyces cerevisiae DNA topoisomerase II. Mol Cell Biol. 1994; 14:3197–207. [PubMed: 8164675]
49. Roca J. The path of the DNA along the dimer interface of topoisomerase II. J Biol Chem. 2004; 279:25783–8. [PubMed: 15047688]
50. Baird CL, Harkins TT, Morris SK, Lindsley JE. Topoisomerase II drives DNA transport by hydrolyzing one ATP. Proc Natl Acad Sci U S A. 1999; 96:13685–90. [PubMed: 10570133]
51. Osheroff N. Eukaryotic topoisomerase II. Characterization of enzyme turnover. J Biol Chem. 1986; 261:9944–50. [PubMed: 3015913]
52. Tingey AP, Maxwell A. Probing the role of the ATP-operated clamp in the strand-passage reaction of DNA gyrase. Nucleic Acids Res. 1996; 24:4868–73. [PubMed: 9016655]
53. Li W, Wang JC. Footprinting of yeast DNA topoisomerase II lysyl side chains involved in substrate binding and interdomainal interactions. J Biol Chem. 1997; 272:31190–5. [PubMed: 9388273]
54. Choudhary C, et al. Lysine acetylation targets protein complexes and co-regulates major cellular functions. Science. 2009; 325:834–40. [PubMed: 19608861]
55. Bates AD, Berger JM, Maxwell A. The ancestral role of ATP hydrolysis in type II topoisomerases: prevention of DNA double-strand breaks. Nucleic Acids Res. 2011; 39:6327–39. [PubMed: 21525132]
56. Ali MM, et al. Crystal structure of an Hsp90-nucleotide-p23/Sba1 closed chaperone complex. Nature. 2006; 440:1013–7. [PubMed: 16625188]
57. Gellert M, Mizuuchi K, O'Dea MH, Nash HA. DNA gyrase: an enzyme that introduces superhelical turns into DNA. Proc Natl Acad Sci U S A. 1976; 73:3872–6. [PubMed: 186775]

58. Lee S, et al. DNA cleavage and opening reactions of human topoisomerase IIalpha are regulated via Mg2+-mediated dynamic bending of gate-DNA. Proc Natl Acad Sci U S A. 2012; 109:2925–30. [PubMed: 22323612]
59. Skouboe C, et al. A human topoisomerase II alpha heterodimer with only one ATP binding site can go through successive catalytic cycles. J Biol Chem. 2003; 278:5768–74. [PubMed: 12480934]
60. Gottler T, Klostermeier D. Dissection of the nucleotide cycle of B. subtilis DNA gyrase and its modulation by DNA. J Mol Biol. 2007; 367:1392–404. [PubMed: 17320901]
61. Deweese JE, Burgin AB, Osheroff N. Using 3′-bridging phosphorothiolates to isolate the forward DNA cleavage reaction of human topoisomerase IIalpha. Biochemistry. 2008; 47:4129–40. [PubMed: 18318502]
62. Otwinowski Z, Minor W. Processing of X-ray diffraction data collected in oscillation mode. Methods Enzymol. 1997; 276:307–326.
63. McCoy AJ, et al. Phaser crystallographic software. J Appl Crystallogr. 2007; 40:658–674. [PubMed: 19461840]
64. Emsley P, Lohkamp B, Scott WG, Cowtan K. Features and development of Coot. Acta Crystallogr D Biol Crystallogr. 2010; 66:486–501. [PubMed: 20383002]
65. Adams PD, et al. PHENIX: a comprehensive Python-based system for macromolecular structure solution. Acta Crystallogr D Biol Crystallogr. 2010; 66:213–21. [PubMed: 20124702]
66. Chen VB, et al. MolProbity: all-atom structure validation for macromolecular crystallography. Acta Crystallogr D Biol Crystallogr. 2010; 66:12–21. [PubMed: 20057044]
67. The PyMOL Molecular Graphics System, Version 1.5.0.1 Schrödinger, LLC.

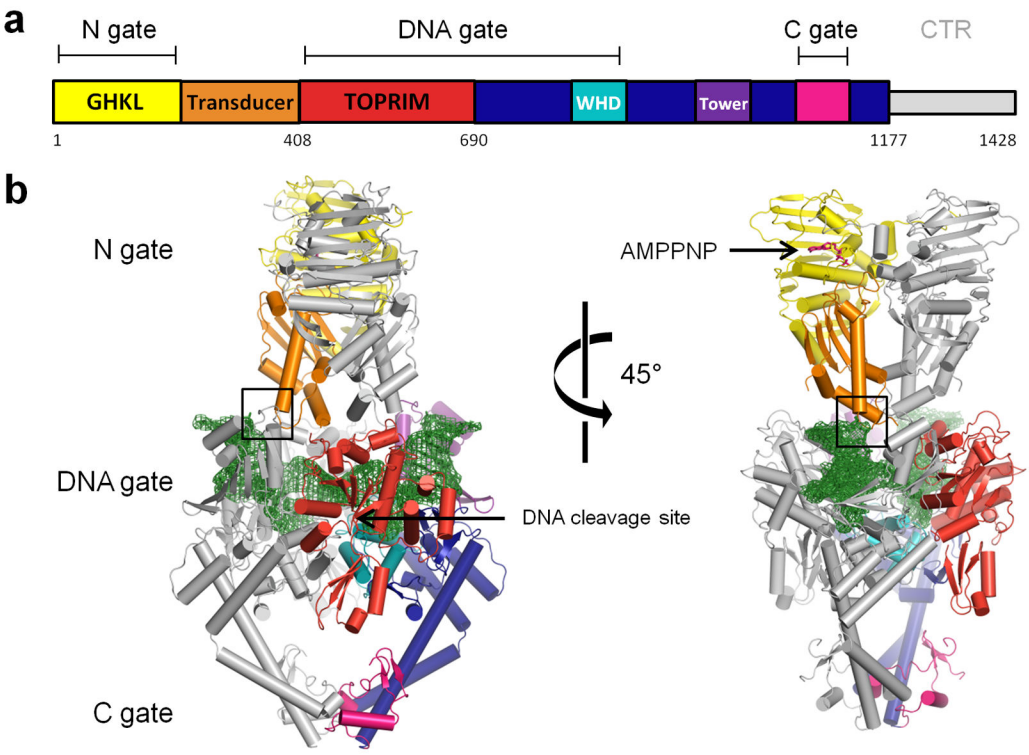

Figure 1. Structure of topo II bound to DNA and AMPPNP

(a) Domain arrangement of type IIA topoisomerases. Functional regions are colored and labeled.

(b) Model of the ternary complex. One topo II protomer is shaded gray, the other colored as in (**a**). $2F_o-F_c$ density (1.5σ contour, green) is shown around the DNA (green sticks).

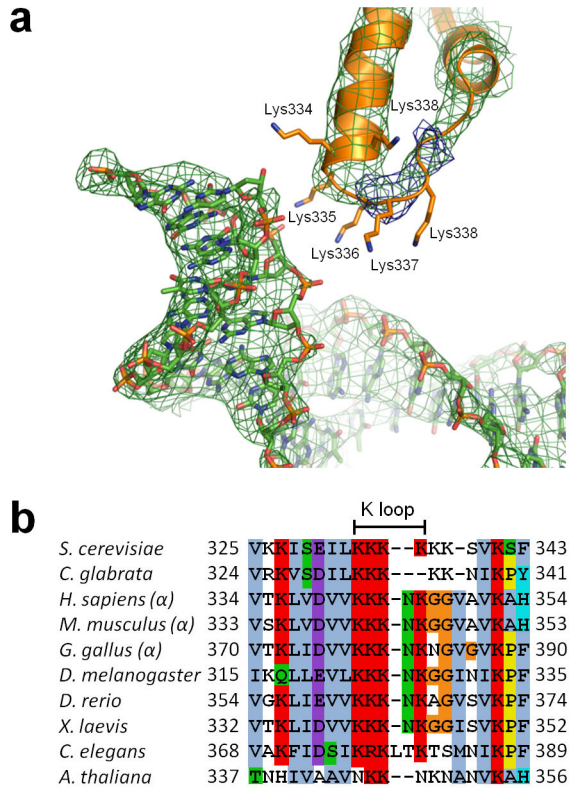

Figure 2. The topo II ATPase domain appears to engage bound DNA

(a) Close-up of the K-loop interaction with DNA. View corresponds to the boxed region in Fig. 1b. DNA is surrounded by 2*Fo*−*Fc* density contoured to 1.5σ. The K-loop is surrounded by 2*Fo*−*Fc* density, contoured to 1.0σ (green), as well as original *Fo*−*Fc* density from the initial MR solution contoured to 2.5σ (blue). The original search model had a gap spanning residues 335–339.

(b) Sequence alignment of eukaryotic type IIA topoisomerases. The K-loop lysines are bracketed. The human, mouse, and chicken sequences correspond to the alpha isoforms; topo IIβ isoforms also bear K-loop lysines.

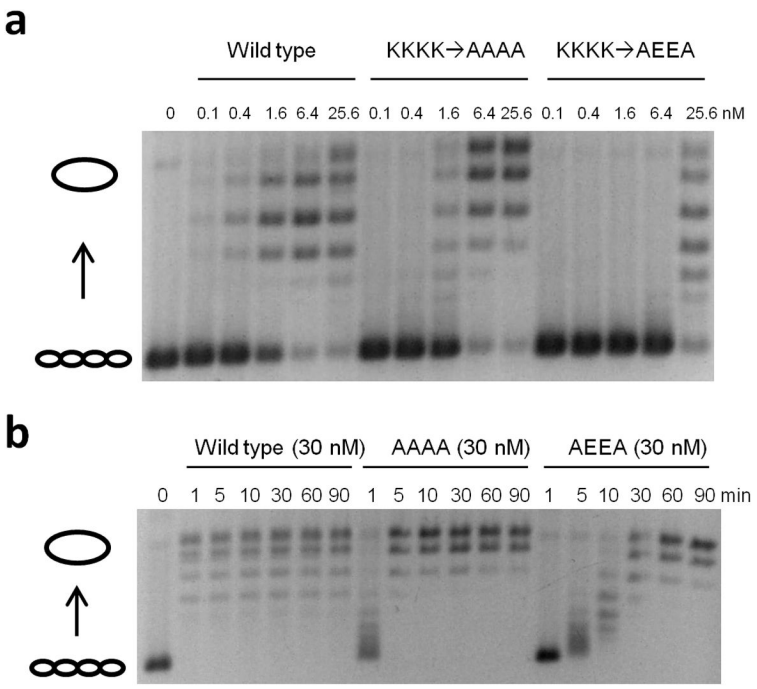

Figure 3. K-loop mutants are deficient at relaxing negatively-supercoiled DNA

(a) Concentration-dependent relaxation of negatively-supercoiled DNA. Supercoiled and relaxed topoisomers are denoted with coiled and open circles, respectively.

(b) Timecourse-dependent negative supercoil relaxation. 7.5 nM DNA is present in both sets of reactions.

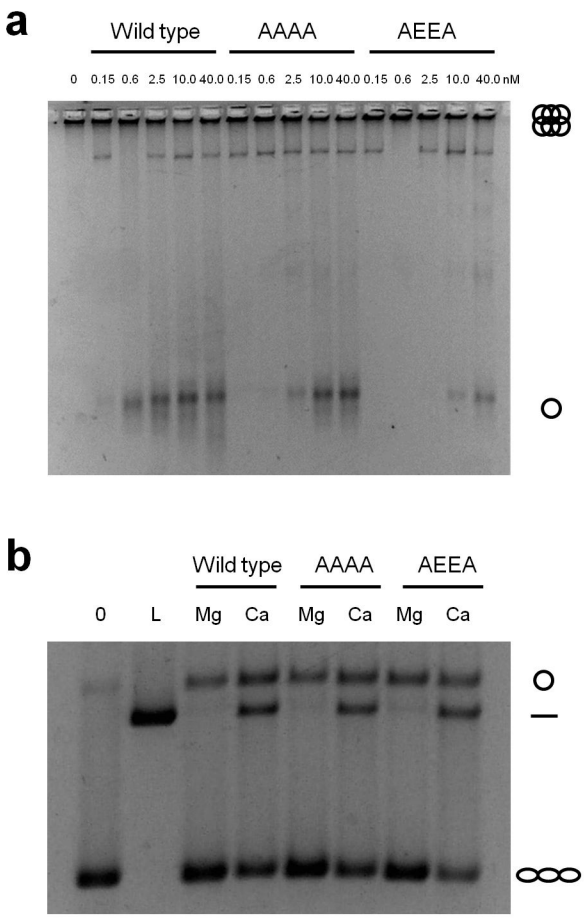

Figure 4. K-loop mutants are defective for decatenation but not DNA cleavage

(a) Decatenation assay. The degree to which the AAAA and AEEA mutants are impaired in decatenation activity follows the trend seen for the relaxation of negatively-supercoiled DNA.

(b) Cleavage assay. Left lane, negative control, no protein. L, plasmid linearized by BamHI. The WT and K-loop mutants show similar propensities to cleave DNA in a calcium-dependent manner.

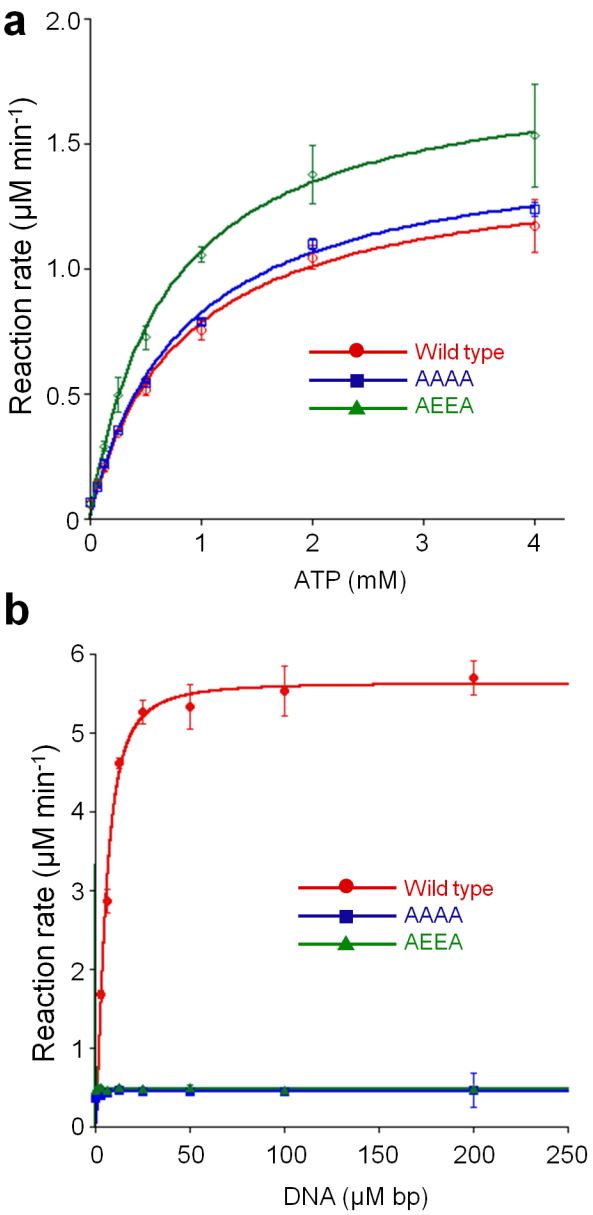

Figure 5. K-loop mutants maintain basal ATPase rates but lose DNA-stimulation of ATP hydrolysis

(a) Basal ATPase activity. Wild-type and K-loop mutant activities are plotted as a function of ATP concentration and fit to a standard Michaelis–Menten kinetic model. Apparent V_{max} values of 1.42 ± 0.06, 1.51 ± 0.06, and 1.82 ± .05 μM min^{-1} were calculated for WT, AAAA, and AEEA topo II constructs, respectively. Calculated K_M values were 0.82 ± 0.09, 0.84 ± 0.09, and 0.70 ± 0.05 mM ATP, respectively.

(b) DNA-stimulated ATPase activity. Wild-type and K-loop mutant activities are monitored at a constant starting concentration of ATP, and are plotted as a function of sheared salmon-sperm DNA concentration.

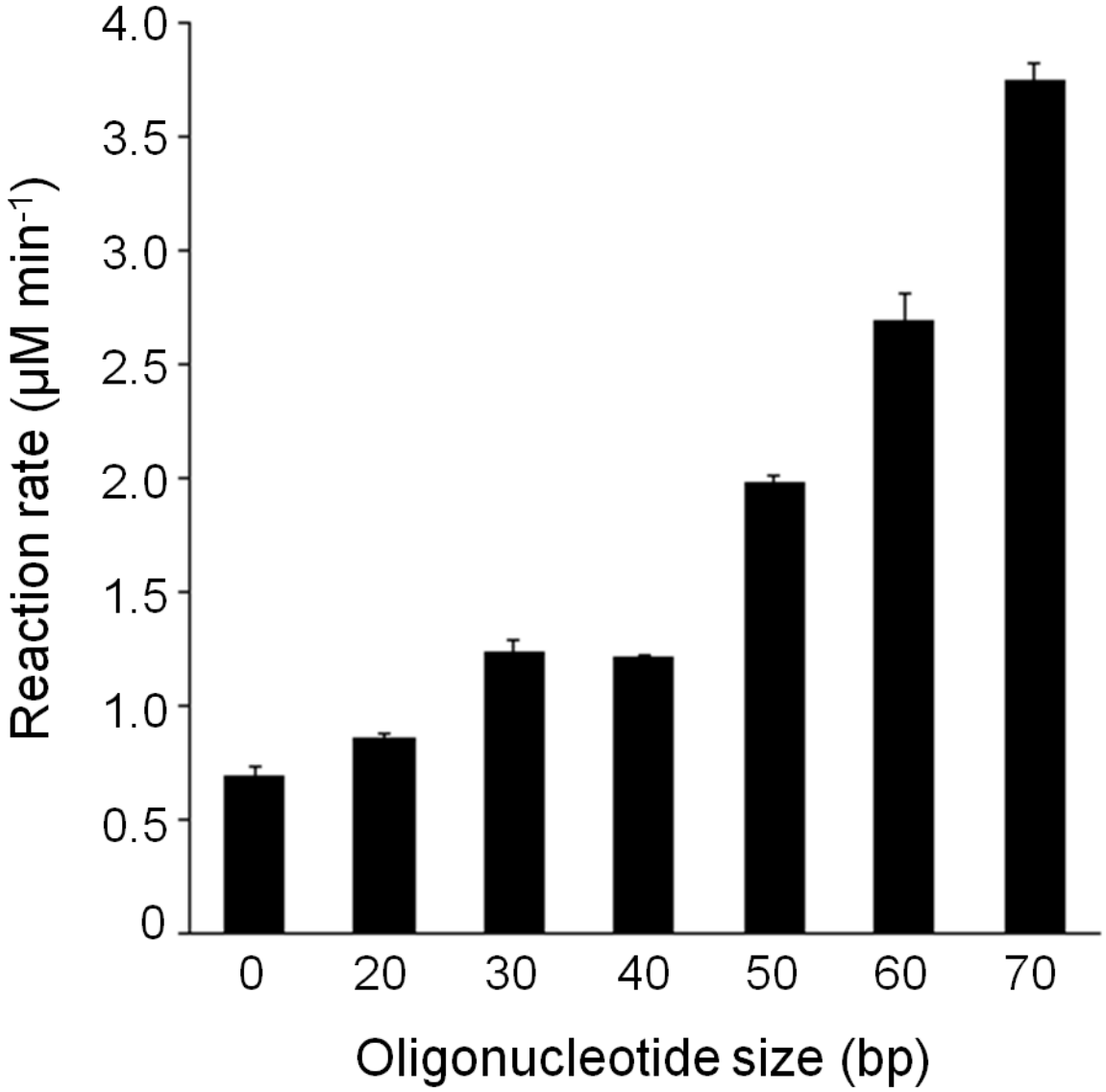

Figure 6. Oligonucleotides stimulate ATP hydrolysis in a length-dependent manner

A 20mer oligonucleotide fails to stimulate ATP hydrolysis beyond the basal rate. As length increases, ATPase stimulation increases. The molar ratio of DNA:protein is 250:1 for these data, and error bars derive from an average of three independent experiments.

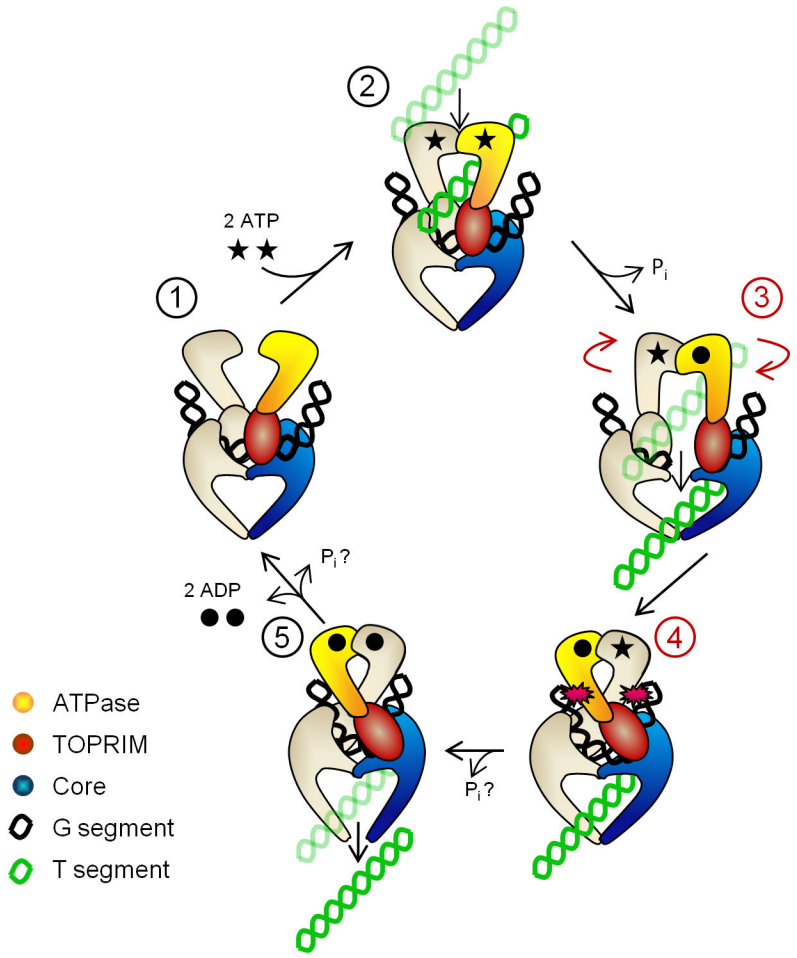

Figure 7. Unexpected complexities in the type IIA topoisomerase catalytic cycle

(1) Homodimer at the beginning of cycle. One monomer is shaded grey and the other is colored as indicated in the key. The enzyme binds and bends a G-segment (black). (2) The binding of two ATP (stars) promotes T-segment capture (green). (3) Hydrolysis of one ATP to ADP (circle) leads to G-segment cleavage and T-segment transport through the break. Following strand transport the ATPase domains swivel about each other to impede backward translocation of the T-segment. (4) G-segment ends are brought back together for religation. K-loop contacts are proposed to trigger hydrolysis of the second ATP. (5) T-segment escape, followed by ADP release, resets the enzyme. Steps (3) and (4) are highlighted in red to denote the new findings from this work; as many prokaryotic type IIA topoisomerases appear to lack a K-loop (Supplementary Fig. 8), interactions between this region and G-segment DNA (step 4) may be limited to eukaryotic topo II homologs. The precise point of P_i release following the second hydrolysis step is not known (question marks).

Table 1

Data collection and refinement statistics

	Topo II-DNA-AMPPNP
Data collection	
Space group	$P2_12_12_1$
Cell dimensions	
a, *b*, *c* (Å)	169.14, 169.88, 169.21
α, β, γ(°)	90, 90, 90
Resolution (Å)	50-4.4 (4.57-4.41)
R_{sym}	7.6 (70.3)
$I / \sigma I$	15.5 (2.0)
Completeness (%)	91.7 (92.9)
Redundancy	4.3 (4.2)
Refinement	
Resolution (Å)	50-4.4
No. reflections	28660
R_{work}/R_{free}	23.9/27.5
No. atoms	
Protein	18050
DNA	2118
AMPPNP	62
Mg	2
B-factors	
Protein	238.5
DNA	278.7
AMPPNP	233.4
Mg	115.1
R.m.s. deviations	
Bond lengths (Å)	0.004
Bond angles (°)	0.842

*Values in parentheses are for highest-resolution shell.